



Elastic Electron Scattering From ^{52}Cr , ^{58}Fe and ^{64}Ni Nuclei in the Framework of the Coherent Density Fluctuation Model

Ahmed N. Abdullah*

Department of Physics, College of Science, University of Baghdad, Baghdad, Iraq

Abstract:

Coherent density fluctuation model (CDFM) has been used to calculate the proton momentum distributions (PMD) and elastic electron scattering form factors, $F(q)$, of the ground state for some even mass nuclei of fp -shell, such as ^{52}Cr , ^{58}Fe and ^{64}Ni nuclei. Both of the PMD and $F(q)$ have been expressed in terms of the weight function $(|f(x)|^2)$ which is determined by means of the charge density distributions (CDD) of the nuclei and determined from theory and experiment. The feature of the long-tail behavior at high momentum region of the PMD's has been obtained by both the theoretical and experimental weight functions. The calculated form factors of these nuclei are in reasonable agreement with those of the experimental data.

Keywords: Proton momentum distributions, Charge density distributions, Coherent density fluctuation model.

الاستطارة الالكترونية المرنة من النوى ^{52}Cr ، ^{58}Fe و ^{64}Ni باستخدام نموذج تموج الكثافة المترابط

أحمد نجم عبدالله*

قسم الفيزياء، كلية العلوم، جامعة بغداد، بغداد، العراق

الخلاصة

تم استخدام نموذج تموج الكثافة المترابط في حساب كل من توزيعات زخم البروتون (PMD) للحالة الارضية وعوامل التشكل $F(q)$ للاستطارة الالكترونية المرنة لبعض النوى الزوجية الواقعة ضمن القشرة النووية fp مثل ^{52}Cr ، ^{58}Fe و ^{64}Ni . لقد تم التعبير عن كل من PMD و $F(q)$ بدلالة دالة التموج $(|f(x)|^2)$ التي تحسب بواسطة توزيعات كثافة الشحنة (CDD). في هذه الدراسة تم حساب دالة التموج من خلال النتائج النظرية والعملية لتوزيعات كثافة الشحنة. تميزت نتائج توزيعات زخم البروتون (المستندة على دالة التموج النظرية والعملية) بخاصية الذيل الطويل عند قيم الزخم العالية. أظهرت هذه الدراسة بان النتائج النظرية لعوامل التشكل للاستطارة الالكترونية المرنة للنوى ^{52}Cr ، ^{58}Fe و ^{64}Ni والمحسوبة بأنموذج التموج المتشابهة تتفق مع النتائج العملية.

1. Introduction

Electron scattering method is a powerful tool for studying nuclear structure because there are two reasons; the first is that the interaction is known, as the electron interacts electromagnetically with the local charge and current density in the target. Since this interaction is relatively weak, one can make measurement without greatly disturbing the structure of the target. The second advantage of electrons is that for fixed energy loss to the target, one can vary the three-momentum transfer \vec{q} and map out the Fourier transforms of the static and transition densities [1]. With electron scattering one can immediately relate the cross section to the transition matrix elements of the local charge and current density operators and this directly to the structure of the target itself.

*Email: Ahmednajim1979@yahoo.com

The scattering of electrons from a target nucleus can occur in two ways. In one, the nucleus is left in its ground state after the scattering and the energy of the electrons is unchanged. In the other, the scattered electron leaves the nucleus in different excited state and has a final energy reduced from the initial just by the amount taken up by the nucleus in its excited state. These two kinds of processes are referred to elastic and inelastic electron scattering [2,3].

In coherent density fluctuation model (CDFM), which is exemplified by the work of Antonov *et al.* [4-6], the local nucleon density distribution (NDD) and the nucleon momentum distributions (NMD) are simply related and expressed in terms of experimentally obtainable fluctuation function (weight function) $|f(x)|^2$. They [4-6] studied the NMD of (^4He and ^{16}O), ^{12}C and (^{39}K , ^{40}Ca and ^{48}Ca) nuclei using weight functions $|f(x)|^2$ specified by the two parameter Fermi (2PF) NDD [7], the data of Reuter *et al.* [8] and the model independent NDD [8], respectively. It is significant to remark that all above studies, employed the framework of the CDFM, proved a high momentum tail in the NMD. Elastic electron scattering from ^{40}Ca nucleus was also investigated in Ref. [4], where the calculated elastic differential cross sections ($d\sigma/d\Omega$) are in good agreement with those of experimental data.

Recently, Al-Rahmani [9] have studied the PMD and $F(q)$ for 2s-1d shell nuclei using the framework of CDFM and derived an analytical form for the CDD based on the use of the single particle harmonic oscillator wave functions and the occupation number of the states. The derived CDD's, which are applicable throughout the whole 2s-1d shell nuclei, have been used in the CDFM. The calculated PMD and elastic form factors of all considered nuclei have been in very good agreement with experimental data.

The aim of the present work is to extend the calculations of Al-Rahmani [9] to higher shells (such as the 1f-2p shell nuclei) and to derive an analytical expression for the CDD based on the use of the single particle harmonic oscillator wave functions and the occupation numbers of the states. The derived CDD is employed in determining the theoretical weight function $|f(x)|^2$ which is used in the CDFM to study the PMD and elastic form factors for ^{52}Cr , ^{58}Fe and ^{64}Ni nuclei. We shall see later that the theoretical $|f(x)|^2$, based on the derived CDD, is capable to provide information about the PMD and elastic electron scattering form factors as do those of experimental CDD of Ref. [7].

2. Theory

The charge density distribution CDD of one body operator can be written as [10]:

$$\rho_c(r) = \frac{1}{4\pi} \sum_{n\ell} \xi_{n\ell} 2(2\ell + 1) |R_{n\ell}|^2 \quad (1)$$

Where $\xi_{n\ell}$ is the proton occupation probability of the state $n\ell$ ($\xi_{n\ell} = 0$ or 1 for closed shell nuclei and $0 < \xi_{n\ell} < 1$ for open shell nuclei) and $R_{n\ell}$ is the radial part of the single particle harmonic oscillator wave function.

The CDD form of ^{52}Cr , ^{58}Fe and ^{64}Ni nuclei is derived on the assumption that there are filled 1s, 1p and 1d orbitals and the proton occupation numbers in 2s, 1f and 2p orbitals are equal to, respectively, $(2 - \beta_1)$, $(Z - 20 - \beta_2)$ and $(\beta_1 + \beta_2)$ and not to 2, $(Z - 20)$ and 0 as in the simple shell model, where the parameters β_1 and β_2 are the occupation number of higher shells. Using this assumption in Eq. (1), an analytical form for the ground state CDD of ^{52}Cr , ^{58}Fe and ^{64}Ni nuclei is obtained as:

$$\rho_c(r) = \frac{e^{-r^2/b^2}}{\pi^{3/2}b^3} \left\{ 5 - \frac{3}{2}\beta_1 + \left(\frac{11}{3}\beta_1 + \frac{5}{3}\beta_2 \right) \left(\frac{r}{b} \right)^2 + \left(4 - 2\beta_1 - \frac{4}{3}\beta_2 \right) \left(\frac{r}{b} \right)^4 + \left(\frac{4}{21}\beta_2 + \frac{8}{105}(Z - 20) + \frac{4}{15}\beta_1 \right) \left(\frac{r}{b} \right)^6 \right\} \quad (2)$$

where Z is the atomic number, b is the harmonic oscillator size parameter, the parameter β_1 characterizes the deviation of the proton occupation numbers from the prediction of the simple shell

model ($\beta_1 = 0$). The parameter β_2 in Eq. (2) is assumed as a free parameter to be adjusted to obtain agreement with the experimental CDD.

The normalization condition of the $\rho_c(r)$ is given by [9]

$$Z = 4\pi \int_0^{\infty} \rho_c(r) r^2 dr \quad (3)$$

and the mean square radius (MSR) of the considered nuclei is given by [9]

$$\langle r^2 \rangle = \frac{4\pi}{Z} \int_0^{\infty} \rho_c(r) r^4 dr \quad (4)$$

The central CDD, $\rho_c(r=0)$ is obtained from Eq. (2) as

$$\rho_c(0) = \frac{1}{\pi^{3/2} b^3} \left[5 - \frac{3}{2} \beta_1 \right] \quad (5)$$

Then β_1 is obtained from Eq. (5) as

$$\beta_1 = \frac{2}{3} (5 - \rho_c(0) \pi^{3/2} b^3) \quad (6)$$

Substituting Eq. (2) into Eq. (4) and after simplification gives:

$$\langle r^2 \rangle = \frac{b^2}{Z} \left(\frac{9Z - 60}{2} + \beta_1 \right) \quad (7)$$

In Eq's (5) and (7), the values of the central density $\rho_c(0)$ and $\langle r^2 \rangle$ are taken from the experiments while the parameter b is chosen in such a way as to reproduce the experimental root mean square radii of nuclei. The PMD, $n(k)$, of the considered nuclei is studied using two distinct methods. In the first, it is determined by the shell model using the single particle harmonic oscillator wave functions in momentum representation and is given by [11]:

$$n(k) = \frac{b^3}{\pi^{3/2}} e^{-b^2 k^2} \left[5 + 4(bk)^4 + (Z - 20) \frac{4}{105} (bk)^6 \right] \quad (8)$$

k is the momentum of the particle.

Whereas in the second method, the $n(k)$ is determined by the Coherent Density Fluctuation Model (CDFM), where the mixed density is given by [4,5]

$$\rho(r, r') = \int_0^{\infty} |f(x)|^2 \rho_x(r, r') dx \quad (9)$$

where:

$$\rho_x(r, r') = 3\rho_0(x) \frac{j_1(k_F(x)|\bar{r} - \bar{r}'|)}{k_F(x)|\bar{r} - \bar{r}'|} \theta(x - \frac{1}{2}|\bar{r} + \bar{r}'|) \quad (10)$$

is the density matrix for Z protons uniformly distributed in a sphere with radius x and density $\rho_0(x) = 3Z / 4\pi x^3$. The Fermi momentum is defined as [4,5]:

$$k_F(x) = \left(\frac{3\pi^2}{2} \rho_0(x) \right)^{1/3} \equiv \frac{V}{x}; \quad V = \left(\frac{9\pi Z}{8} \right)^{1/3} \quad (11)$$

and the step function θ , is defined by

$$\theta(y) = \begin{cases} 1, & y \geq 0 \\ 0, & y < 0 \end{cases} \quad (12)$$

The diagonal element of Eq. (9) gives the one-particle density as

$$\rho_c(r) = \rho_c(r, r')|_{r=r'} = \int_0^{\infty} |f(x)|^2 \rho_x(r) dx \quad (13)$$

In Eq. (13), $\rho_x(r)$ and $|f(x)|^2$ have the following forms [4,5]:

$$\rho_x(r) = \rho_0(x)\theta(x-r) \quad (14)$$

$$|f(x)|^2 = \frac{-1}{\rho_0(x)} \frac{d\rho(r)}{dr} \Big|_{r=x} \quad (15)$$

The weight function of Eq. (15), determined in terms of the CDD satisfies the following normalization condition [4,5]

$$\int_0^{\infty} |f(x)|^2 dx = 1, \quad (16)$$

and holds for monotonically decreasing density CDD distribution, i.e. $\frac{d\rho(r)}{dr} < 0$.

On the basis of eq. (13), the PMD, $n(k)$, is expressed as [4,5]:

$$n(k) = \int_0^{\infty} |f(x)|^2 n_x(k) dx, \quad (17)$$

where

$$n_x(k) = \frac{4}{3} \pi x^3 \theta(k_F(x) - |\vec{k}|), \quad (18)$$

is the Fermi-momentum distribution of the system with density $\rho_0(x)$. By means of Eqs. (15), (17) and (18), an explicit form for the PMD is expressed in terms of $\rho_c(r)$ as

$$n_{CDFM}(k) = \left(\frac{4\pi}{3}\right)^2 \frac{4}{Z} \int_0^{V/k} 6\rho_c(x)x^5 dx - \left(\frac{V}{k}\right)^6 \rho_c\left(\frac{V}{k}\right), \quad (19)$$

with normalization condition

$$Z = \int n_{CDFM}(k) \frac{d^3k}{(2\pi)^3} \quad (20)$$

The elastic monopole form factor $F(q)$ of the target nucleus is also expressed in the CDFM as [4,5]:

$$F(q) = \frac{1}{Z} \int_0^{\infty} |f(x)|^2 F(q, x) dx \quad (21)$$

where $F(q, x)$ is the form factor of uniform charge density distribution given by:

$$F(q, x) = \frac{3Z}{(qx)^2} \left[\frac{\sin(qx)}{(qx)} - \cos(qx) \right] \quad (22)$$

Inclusion the corrections of the nucleon finite size $F_{fs}(q)$ and the center of mass corrections $F_{cm}(q)$ in the calculations requires multiplying the form factor of equation (21) by these corrections. Here, $F_{fs}(q)$ is considered as free nucleon form factor which is assumed to be the same for protons and neutrons. This correction takes the form [12]:

$$F_{fs}(q) = e^{\left(\frac{-0.43q^2}{4}\right)} \quad (23)$$

The correction $F_{cm}(q)$ removes the spurious state arising from the motion of the center of mass when shell model wave function is used and given by [12]:

$$F_{cm}(q) = e^{\left(\frac{b^2 q^2}{4A}\right)} \quad (24)$$

It is important to point out that all physical quantities studied above in the framework of the CDFM such as PMD and $F(q)$, are expressed in terms of the weight function $|f(x)|_{th}^2$. Therefore, it is worthwhile trying to obtain the weight function firstly from the CDDs of two parameter Fermi (2PF) and three parameter Fermi (3PF) models extracted from the analysis of elastic electron-nuclei scattering experiments and secondly from theoretical considerations. The CDDs of 2PF and 3PF, respectively are given by [7]

$$\rho_c(r) = \frac{\rho_0}{1 + e^{(r-c)/z}} \quad (25a)$$

$$\rho_c(r) = \frac{\rho_0(1 + wr^2/c^2)}{1 + e^{(r-c)/z}} \quad (25b)$$

Introducing Eqs. (25) into Eq. (15), we obtain the experimental weight function $|f(x)|_{2PF}^2$ and

$|f(x)|_{3PF}^2$ as

$$|f(x)|_{2PF}^2 = \frac{4\pi x^3 \rho_0}{3A z} \left(1 + e^{\frac{x-c}{z}}\right)^{-2} \exp\left(\frac{x-c}{z}\right) \quad (26a)$$

$$|f(x)|_{3PF}^2 = \frac{4\pi x^3 \rho_0}{3A} \left(\frac{\left(1 + \frac{wx^2}{c^2}\right) \left(1 + e^{\frac{x-c}{z}}\right)^{-2} e^{\frac{x-c}{z}}}{z} - \frac{2wx \left(1 + e^{\frac{x-c}{z}}\right)^{-1}}{c^2} \right) \quad (26b)$$

Moreover, introducing the derived CDD of Eq. (2) into Eq. (15), we obtain the theoretical weight function $|f(x)|_{th}^2$ as

$$|f(x)|_{th}^2 = \frac{8\pi x^4}{3Zb^2} \rho_c(x) - \frac{16x^4}{3Z\pi^{1/2}b^5} \left[\frac{11}{6} \beta_1 + \frac{5}{6} \beta_2 + \left(4 - 2\beta_1 - \frac{4}{3} \beta_2\right) \left(\frac{x}{b}\right)^2 + \left(\frac{4}{35} (Z - 20) + \frac{2}{5} \beta_1 + \frac{2}{7} \beta_2\right) \left(\frac{x}{b}\right)^4 \right] e^{-x^2/b^2} \quad (27)$$

3. Results and Discussion

The proton momentum distribution, $n(k)$, and elastic electron scattering form factors, $F(q)$, for ^{52}Cr , ^{58}Fe and ^{64}Ni nuclei are studied by means of the CDFM. The distribution $n(k)$ of Eq. (19) is calculated in terms of the CDD obtained firstly from theoretical consideration as in Eq. (2) and secondly from experiments, such as, 2PF and 3PF [7]. The harmonic oscillator size parameter b is chosen such that to reproduce the measured root mean square radii (r_{ms}) of nuclei under study and the parameter β_1 is determined by introducing the chosen value of b and the experimental central density $\rho_{exp}(0)$ into Eq. (6), while the parameter β_2 is assumed as a free parameter to be adjusted to obtain agreement with the experimental CDD. It is important to remark that when $\beta_1 = \beta_2 = 0$, Eq.(2) is reduced to that of the simple shell model prediction. The values of the harmonic oscillator size parameter b and the calculated parameters of β_1 and β_2 together with the other parameters employed in the present calculations for nuclei under study are listed in Table-1. The calculated occupation numbers of protons in the orbitals 2s, 1f, and 2p, which are equal to $(2 - \beta_1)$, $(Z - 20 - \beta_2)$ and $(\beta_1 + \beta_2)$, respectively, of the considered nuclei are displayed in Table 2. The calculated rms $\langle r^2 \rangle_{cal}^{1/2}$ and those

of experimental data $\langle r^2 \rangle_{\text{exp}}^{1/2}$ [7] are displayed in this table as well for comparison. The comparison shows a remarkable agreement between $\langle r^2 \rangle_{\text{cal}}^{1/2}$ and $\langle r^2 \rangle_{\text{exp}}^{1/2}$ for all considered nuclei.

Table 1- Parameters for the CDD of the considered nuclei

Nuclei	Z	Model [7]	w	c (fm)	z (fm)	$\rho_{\text{exp}}(0)$ (fm^{-3}) [7]	b (fm)	β_1	β_2
^{52}Cr	24	2PF	----	4.01	0.487	0.0775185	2.046	0.867192	0.281153
^{58}Fe	26	2PF	----	4.027	0.576	0.0790024	2.059	0.771767	0.598975
^{64}Ni	28	3PF	-0.2284	4.5211	0.5278	0.0777104	2.104	0.644818	0.921457

Table 2- Calculated occupation numbers of 2s, 1f, and 2p orbitals of the considered nuclei together with $\langle r^2 \rangle_{\text{cal}}^{1/2}$ and $\langle r^2 \rangle_{\text{exp}}^{1/2}$

Nuclei	Occupation No. of 2s ($2 - \beta_1$)	Occupation No. of 1f ($Z - 20 - \beta_2$)	Occupation No. of 2p ($\beta_1 + \beta_2$)	$\langle r^2 \rangle_{\text{cal}}^{1/2}$ (fm)	$\langle r^2 \rangle_{\text{exp}}^{1/2}$ (fm) [7]
^{52}Cr	1.132808	3.718847	1.148345	3.70	3.684
^{58}Fe	1.228233	5.401025	1.370742	3.783	3.783
^{64}Ni	1.355182	7.7078543	1.566275	3.908	3.907

The dependence of the CDD's (in fm^{-3}) on r (in fm) for ^{52}Cr , ^{58}Fe and ^{64}Ni nuclei is shown in Figure-1. The blue and red curves are the calculated results using Eq. (2) with $\beta_1 = \beta_2 = 0$ and $\beta_1 \neq \beta_2 \neq 0$, respectively whereas the filled circle symbols correspond to the experimental data [7]. This figure shows that the blue curves are in poor agreement with the experimental data, especially for small r . Inclusion of the parameters β_1 and β_2 (i.e., considering the higher orbitals) in the calculation leads to a very good agreement with the experimental data as demonstrated by the red curves.

The dependence of $n(k)$ (in fm^3) on k (in fm^{-1}) for ^{52}Cr , ^{58}Fe and ^{64}Ni nuclei is shown in Figure-2. The blue curves are the calculated $n(k)$ of Eq. (8) obtained by the shell model calculation using the single particle harmonic oscillator wave functions in momentum representation. The filled circle symbols and red curves are the $n(k)$ obtained by the CDFM of Eq. (19) using the experimental and theoretical CDD, respectively. It is clear that the behavior of the blue curves obtained by the shell model calculations is in contrast with those reproduced by the CDFM. The important feature of the blue distributions is the steep slope behavior when k increases. This behavior is in disagreement with the studies [4, 5, 13- 15] and it is attributed to the fact that the ground state shell model wave function given in terms of a Slater determinant does not take into account the important effect of the short range dynamical correlation functions. Hence, the short-range repulsive features of the nucleon-nucleon forces are responsible for the high momentum behavior of the $n(k)$ [14, 15]. It is noted that the general structure of the filled circle symbols and red curves at the region of high momentum components is almost the same for ^{52}Cr , ^{58}Fe and ^{64}Ni nuclei, where these curves have the property of long tail manner at momentum region $k \geq 2 \text{ fm}^{-1}$. The property of long-tail manner obtained by the CDFM, which is in agreement with the studies [4, 5, 13- 15], is connected to the presence of high densities $\rho_x(r)$ in the decomposition of Eq. (14), though their fluctuation functions $|f(x)|^2$ are small.

The dependence of elastic electron scattering form factors $F(q)$ on the momentum transfer q (in fm^{-1}) for considered nuclei is shown in Figure-3. The calculated form factors (solid curves) of ^{52}Cr , ^{58}Fe and ^{64}Ni nuclei, obtained in the framework of CDFM using the theoretical weight function of Eq. (27), are compared with those of experimental data [7,16,17]. As there is no data available for the ^{58}Fe nucleus, we have compared the calculated form factors of this nucleus with those obtained by the Fourier transform of the 3PF density. Figure-3 shows that the diffraction minima and maxima of the considered nuclei are reproduced in the correct places. Both the behavior and the magnitudes of the calculated form factors of these nuclei are in reasonable agreement with those of the experimental data.

4. Conclusions

It is concluded that the derived form of CDD of Eq.(2) employed in the determination of theoretical weight function of Eq. (27) is capable to reproduce information about the $n(k)$ and elastic form factors as do those of the experimental data.

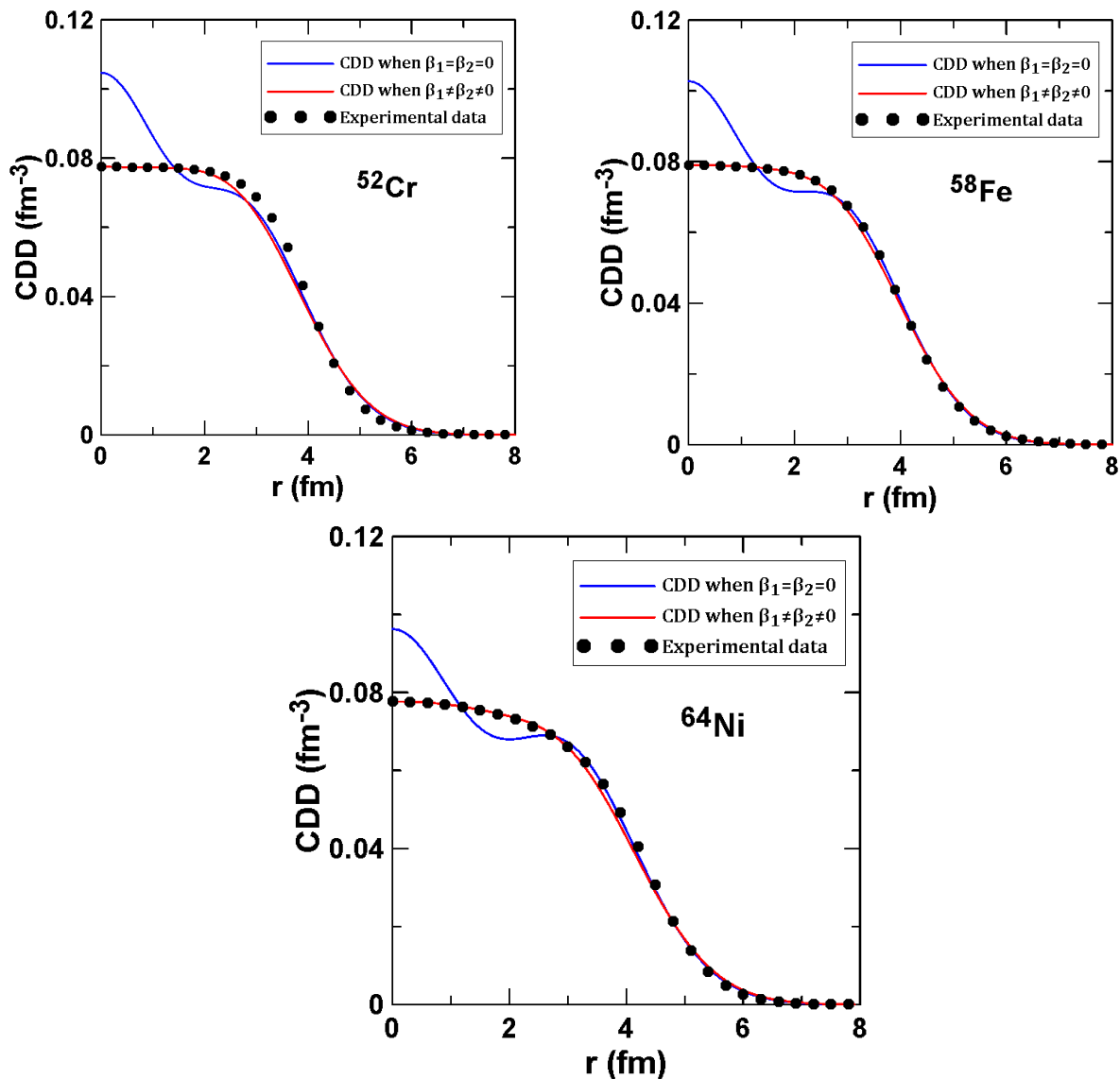


Figure 1- The dependence of the CDD on r for ⁵²Cr, ⁵⁸Fe and ⁶⁴Ni nuclei. The blue and red curves are the calculated CDD of Eq. (2) when $\beta_1 = \beta_2 = 0$ and $\beta_1 \neq \beta_2 \neq 0$, respectively. The filled circle symbols are the experimental data taken from ref. [7].

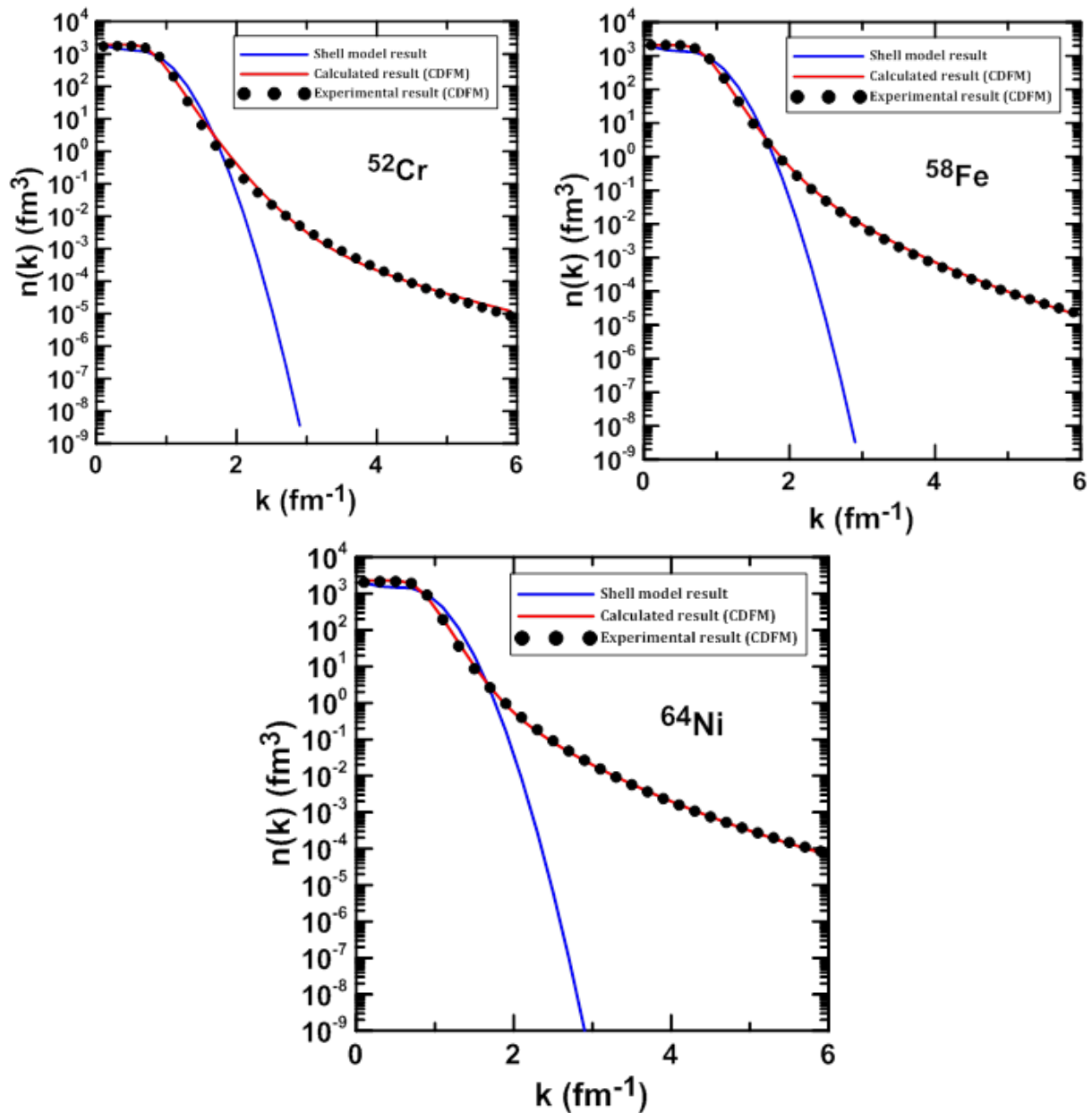


Figure 2-The dependence of $n(k)$ on k for ^{52}Cr , ^{58}Fe and ^{64}Ni nuclei. The red curves and filled circle symbols are the calculated $n(k)$ expressed by the CDFM of Eq. (19) using the theoretical CDD of Eq. (2) and the experimental data of ref. [7], respectively. The blue curves are the calculated $n(k)$ of Eq. (8) obtained by the shell model calculation using the single-particle harmonic oscillator wave functions in momentum representation.

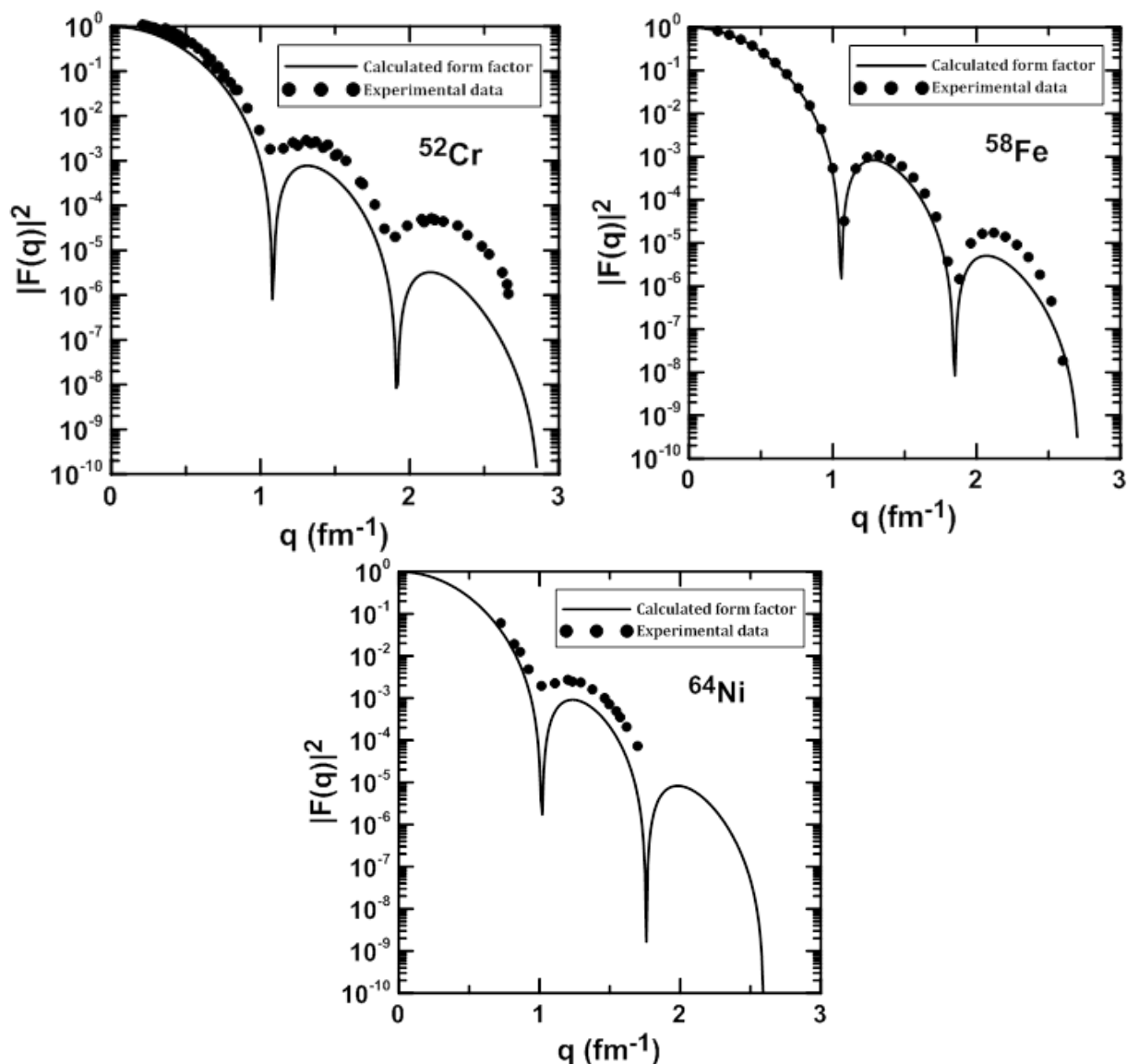


Figure 3- The dependence of the form factors on momentum transfer q for ^{52}Cr , ^{58}Fe and ^{64}Ni nuclei. The solid curves are the form factors calculated using Eq. (21). The experimental data (filled circle symbols) are taken from Refs. [16], [7] and [17] for ^{52}Cr , ^{58}Fe and ^{64}Ni nuclei, respectively.

References

1. Donnelly T.W. and Sick I. **1984**. Elastic magnetic electron scattering from nuclei. *Reviews of Modern Physics*, 56, pp:461-566.
2. Wapstra A. H., Audi G. and Hoekstra R. **1988**. Atomic masses from (mainly) experimental data. *Atomic Data and Nuclear Data Tables*, 39, pp: 281-287.
3. Uberall H. **1970**. *Electron Scattering From Complex Nuclei*, Part A, Academic Press, New York.
4. Antonov A. N., Hodgson P. E. and Petkov I. Z. **1988**. *Nucleon momentum and density distribution in nuclei*. Clarendon, Oxford, pp:1-165.
5. Antonov A. N., Nikolaev V.A. and Petkov I. Z. **1980**. Nucleon momentum and density distributions of nuclei, *Z. Physik*, A 297, pp: 257-260.
6. Antonov A. N., Hodgson P. E. and Petkov I. Z. **1993**. *Nucleon correlation in nuclei*, Springer-Verlag, Berlin-Heidelberg-New York.
7. Vries H. D., Jager C.W., and Vries C. **1987**. Nuclear Charge density distribution parameters from elastic electron scattering. *Atomic data and nuclear data tables*, 36 (3), pp: 495-536.
8. Reuter W., Fricke G., Merle K. and Miska H. **1982**. Nuclear charge distribution and rms radius of C-12 from absolute elastic electron scattering measurements. *Physical Review C* 26, pp: 806-818.
9. Al-Rahmani A. A. **2016**. Elastic Electron Scattering from ^{35}Cl , ^{37}Cl and ^{39}K Nuclei. *International Journal of Science and Research*, 5 (1), pp: 741-747.

10. Flaih G. N., **2008** .The effect of two-body correlation function on the density distributions and electron scattering form factors of some light nuclei. Ph.D. Thesis, University of Baghdad, pp: 1-134.
11. Hassan M. A. **2010**. A study of nuclear momentum distributions and elastic electron scattering form factors for light nuclei using coherent density fluctuation model. M. Sc. Thesis, University of Baghdad, pp:1-80.
12. Hamoudi A. K., Flaiyh G. N. and Abdullah A. N. **2015**. Study of Density Distributions, Elastic Electron Scattering form factors and reaction cross sections of ${}^9\text{C}$, ${}^{12}\text{N}$ and ${}^{23}\text{Al}$ exotic nuclei", *Iraqi Journal of Science*, 56 (1A), pp: 147-161.
13. Moustakidis C. C. and Massen S. E. **2000**. One-body density matrix and momentum distribution in s-p and s-d shell nuclei. *Physical Review*, C 62, pp: 34318_1-34318_7.
14. Traini M. and Orlandini G. **1985** . Nucleon momentum distributions in doubly closed shell nuclei, *Z. Physik*, A 321, pp: 479-484.
15. M. D. Ri, Stringari S. and Bohigas O. **1982**. Effects of short range correlations on one- and two-body properties of nuclei. *Nuclear Physics*, A 376, pp:81-93.
16. Lightbody J. W., Bellicard J. B., Cavedon J. M., Frois B., Goutte D., Huet M., Leconte P., Nakada A., Ho P. X., Platchkov S. K., Turck-Chieze S., de Jager C. W., Lapik'as J. J. and de Witt Huberts P.K. A. **1983**. Elastic and inelastic electron scattering from ${}^{50,52,54}\text{Cr}$. *Physical Review* C27, pp: 113-132.
17. Hamoudi A. K. and Ojaimi H. F. **2014**. Nucleon momentum distributions and elastic electron scattering form factors for ${}^{58}\text{Ni}$, ${}^6\text{Ni}$, ${}^{62}\text{Ni}$ and ${}^{64}\text{Ni}$ isotopes using the framework of coherent fluctuation model. *Iraqi Journal of Physics*, 12(24), pp:33-42.